Egyptian Journal of Animal Health

P-ISSN: 2735-4938 On Line-ISSN: 2735-4946
Journal homepage: https://ejah.journals.ekb.eg/

Antimicrobial, Mechanical and Structural Evaluation of FMWCNTs/PVA nano-composites

Eman H. Ahmed* and Fayza A. Sdeek**

*Polymers and Pigments Department, Chemical Industries Research institute, National Research Centre, 33 El Behooth St., Dokki, Giza, 12622, Egypt

**Pesticide Residues and Environmental Pollution Department, Central Agricultural Pesticide Laboratory, Agricultural Research Center (ARC), Dokki, Giza 12618, Egypt

Received in 24/5/2023
Received in revised from 9/6/2023
Accepted in 29/6/2023

Keywords:
Antimicrobial, multiwalled carbon nanotubes, tensile strength, biological activity

GRAPHICAL ABSRTACT

Functionalized multiwalled carbon nanotubes (FMWNTs) were used in this study to improve the performance of polyvinyl (PVA). The hydrogen-bonding interactions between polyvinyl alcohol and nanofillers provided the driving force for the creation of the homogenous dispersion nanocomposite films between the FMWCNTs into the polymer matrix. Antimicrobial activity, tensile strength tan δ, transmission electron microscopy, thermal gravimetric analysis and Fourier transform infrared were among the techniques used to examine the biological, mechanical and structural performance of the prepared nanocomposite. Because of their homogeneous dispersion across the PVA matrix, the nanofillers considerably improved the film's mechanical and biological activity.

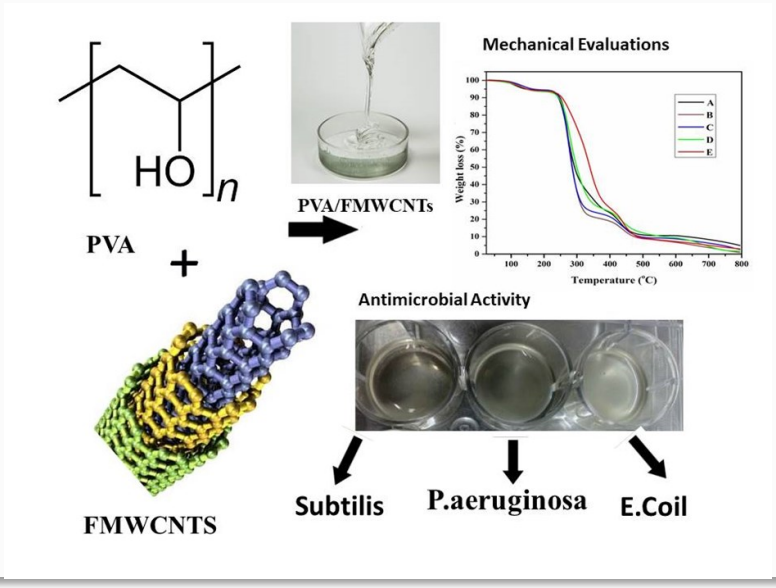

Corresponding author: **Eman H. Ahmed**, Polymers and Pigments Department, Chemical Industries Research institute, National Research Centre, 33 El Behooth St., Dokki, Giza, 12622, Egypt
E-mail address: eman_helmy111@yahoo.com
DOI: 10.21608/ejah.2023.375564

INTRODUCTION

To get really uniform dispersion in their host polymer matrix, FMWCNTs still have to overcome several practical challenges, even though it is viewed as promising nanofiller for the next generation of nanomaterials **(Zhu et al. (2012) and Novaes et al. (2010)**. MWCNT possess a large number of exfoliation readily to form monolayer nanosheets that diffuse gradually in the polymer matrix **(Kuang et al. (2015), Nath et al. (2014) and Uddin et al. (2015)**. These functional groups greatly enhance the dispersion ability in liquids or polymer matrix through covalent or non-covalent bonding **(Stankovich et al.(2007), Bose et al. (2012) and Coleman et al (2004).** The CNTs are bonded vertically to graphene sheets using covalent bonds. As a result, all of the graphene and carbon nanotubes are united into a single unit, producing super-elasticity **(Ribeiro et al. (2021)** and effective electrical connections **(Palumbo et al. (2022)**.

In order to create composite foam with increased specific strength, elasticity, and mechanical stability, entangled CNTs were connecting with the polymer matrix to stop fracture propagation, brittle breakage and increased the stretchability of entangled CNTs to achieve a retractable 200% elongation. Because PVA films are nontoxic, odorless, and biocompatible, they are also attractive candidates for biotechnological applications such tissue engineering, drug delivery, articular cartilage, and biosensors **(Hemalatha et al. (2014)**. Consequently, it has recently attracted a lot of interest from the research community. Studies have demonstrated that PVA hydrogel is a perfect biomaterial for articular cartilage regeneration because of its advantageous biocompatibility and bio-tribological properties. Thus, the aim of this study is to prepare nanocomposite are also considered to be very good options for antimicrobial agent **(Muhammad et al. (2019)**. Thus, they are proposed as novel constituents of antimicrobial wound dressing systems, which can be synthesized by trapping PVA in FMWCNTS **(Abdullah et al.(2016).**

MATERIALS and METHODS

1. Materials

PVA (99% hydrolyzed, Mw ~ 89,000–98,000) were purchased from Sigma–Aldrich. The source of the multiwalled carbon nanotubes was Nanostructured & Amorphous Materials, Inc. USA. The as-received MWCNT material had an outside diameter of 10–20 nm and an interior diameter of 5–10 nm, with a purity of >95%. Hydrochloric acid (37%) was provided Sigma–Aldrich.

2. Preparation of PVA/ FMWCNTs nanocomposites:

The FMWCNTs were treated with hydrochloric acid in an ultrasonication bath (300 W, 40 kHz) for three hours in order to purify them. Several filtrations were performed on the sample to get rid of contaminants. The FMWCNTs were vacuum-dried for one hour at 180 °C.

The following steps describe the preparation of PVA/FMWCNTs nanocomposite films using a solution casting approach. To create a homogeneously dispersed PVA/FMWCNTs solution, (0.1 % based on the total weight of PVA) was diluted in 25 mL DI water and then scattered using ultrasonic (300 W) for 30 minutes. Also, a calculated amount of FMWCNTs was diluted with 25 milliliters of DI water and subjected to a 30-minute sonication. The mixture was then allowed to cool to room temperature. After adding the aqueous suspension gradually to the PVA solution and ultrasonically for five minutes at room temperature, the FMWCNTs aqueous solution was progressively added to the mixture and ultrasonically sonicated for thirty minutes.

The solution was then poured onto a glass plate, allowed to cool at room temperature for 48 hours, and then placed under vacuum at 40 degrees Celsius to create a film until its weight stabilized. The samples were designed as PVA (sample A), PVA/0.1FMWCNTS (sample B),

PVA/0.2 FMWCNTs (C), PVA/ 0.3 FMWCNTs (D), and PVA/04 GO/ 0.5 FFMWCNTs (E), respectively.

RESULTS

As shown in Table (1) DMTA data for pure PVA and its PVA/MWNTs nanocomposites. However Table (2) summarizes a summary of the disc diffusion data for the four samples (A) PVA/0.1 FMWCNTS, (B) PVA/0.2 FMWCNTs, (C) PVA/ 0.3FMWCNTs and (D) (PVA/04 /0.5FFMWCNTs).

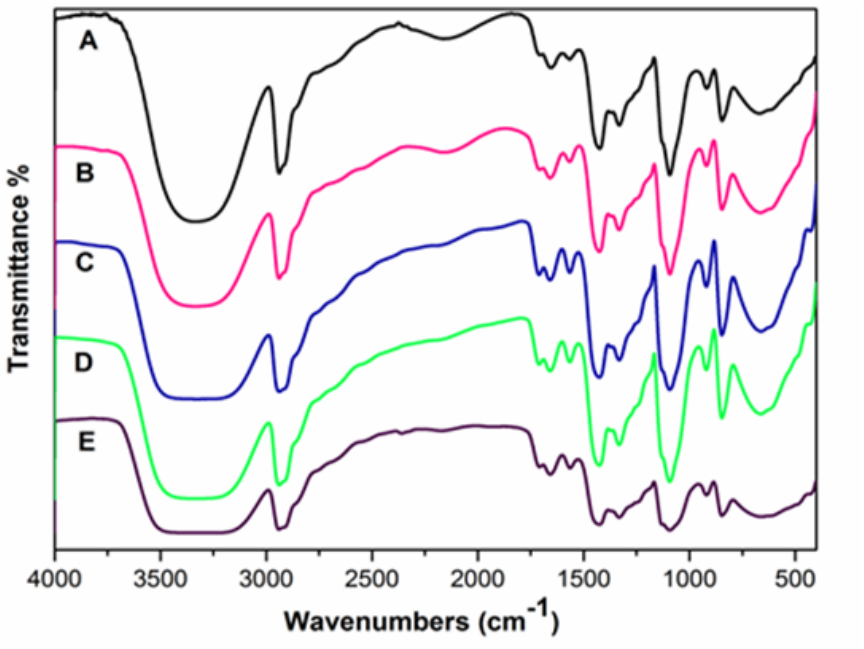

Fig (1) FTIR spectra of (A) PVA , (B) PVA/0.1FMWCNTS , (C) PVA/0.2 FMWCNTs , (D) PVA/ 0.3FMWCNTs and (E) (PVA/04 GO/0.5FFMWCNTs) , respectively.

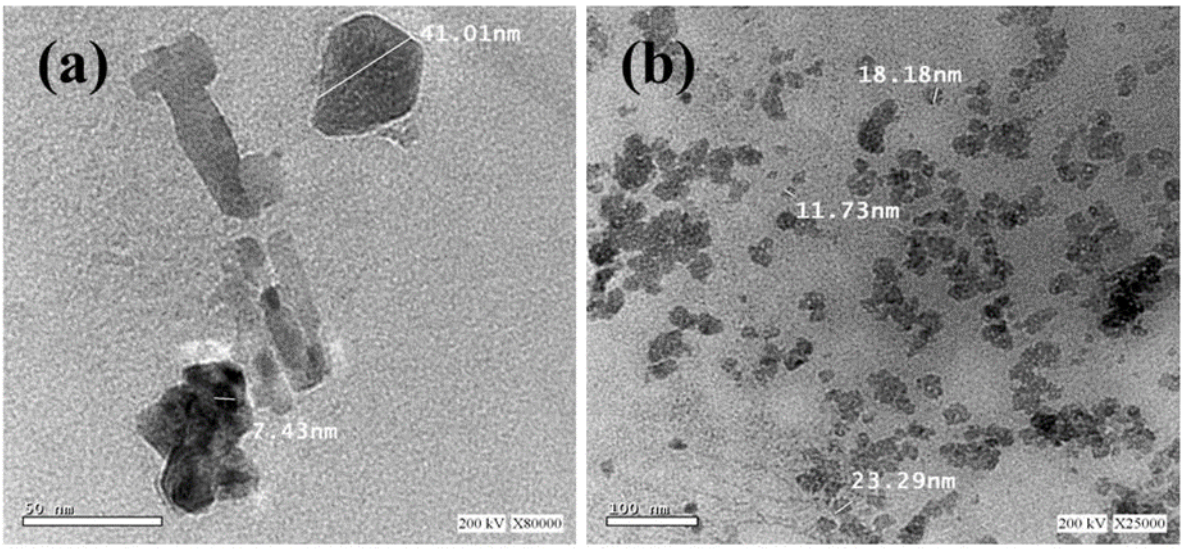

Fig (2) TEM of (a) PVA/0.2 FMWCNTs lower concentration, (b) PVA/ 0.5FMWCNTs higher concentration, respectively.

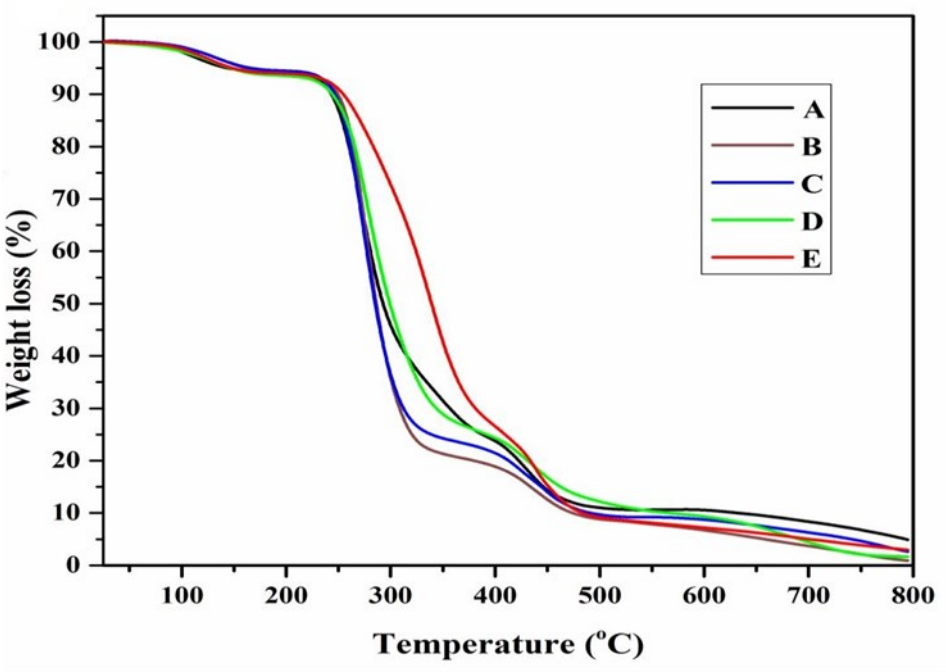

Fig (3) TGA of (A) PVA , (B) PVA/0.1FMWCNTS , (C) PVA/0.2 FMWCNTs , (D) PVA/ 0.3FMWCNTs and (E) (PVA/04 GO/0.5FFMWCNTs) , respectively.

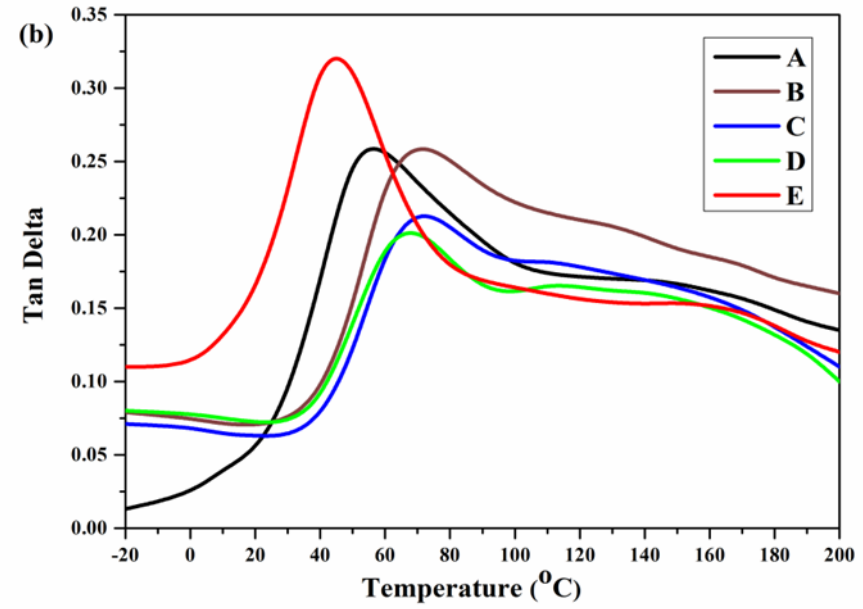

Fig (4) DMA experimental results on (A) PVA, (B) PVA/0.1FMWCNTS, (C) PVA/0.2 FMWCNTs , (D) PVA/ 0.3FMWCNTs and (E) (PVA/04 GO/0.5FFMWCNTs) , respectively

Table 3. Percentage of CLA in camels at Bassatin abattoir during 2020-2022.

Form	No. of examined animals	No. of affected animals	Percentage
Superficial	850	83	9.76%
Visceral		5	0.58%
Total		88	10.35%

Superficial form is significantly ($p < 0.00001$) prevalent than visceral form.

Clinical findings:

Out of the 850 examined animals at Bassatin abattoir, 83 were affected by superficial form of CLA. The affected animals had showed enlargement of different superficial LNs with a distinct variation in size ranging from small lemon up to orange size or even larger

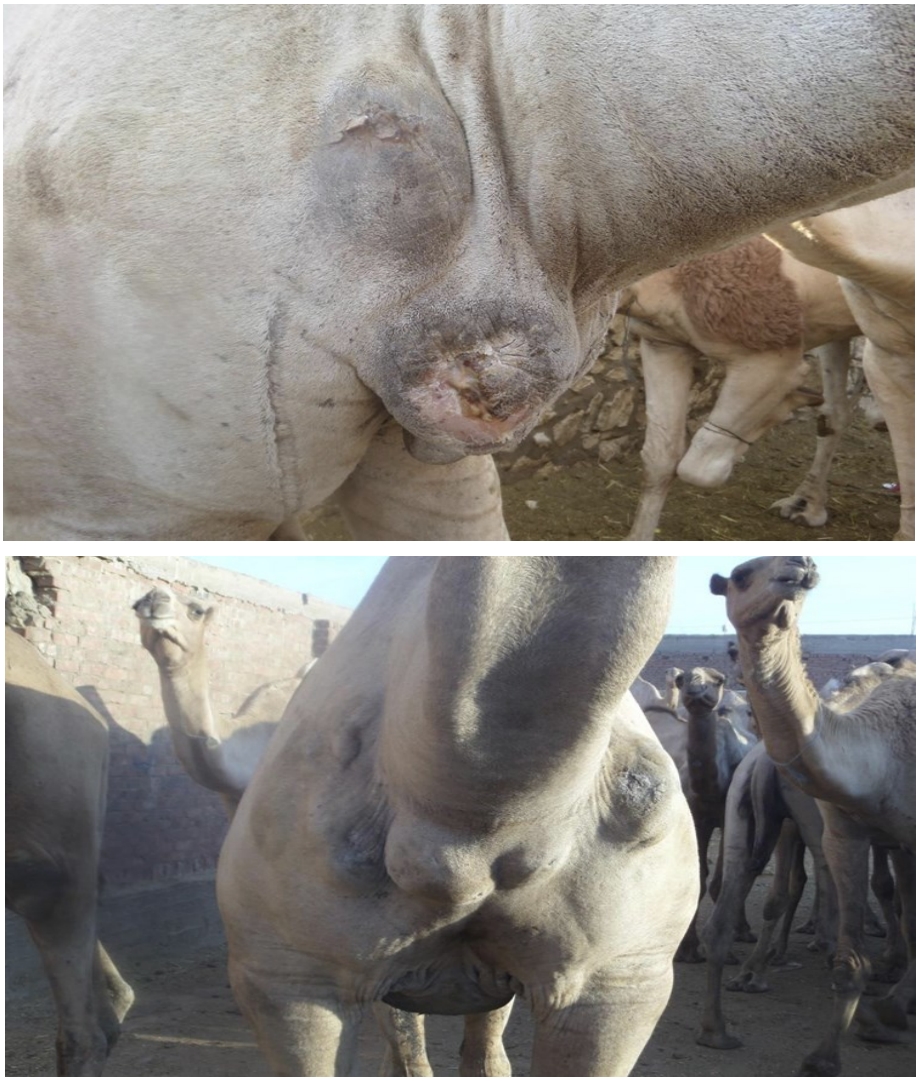

Fig. (1): CLA in camel involving both inferior cervical and both prescapular LNs with ulceration of outer skin .

Table (1): DMTA data for pure PVA and its PVA/MWNTs nanocomposites.

Emulsion	Storage Modulus (MPa) At 20°C	Relaxation Strength	T_g^b (°C)
A	1850	0.263	54.1
B	6750	0.259	68.4
C	7700	0.223	69.1
D	4950	0.212	65.9
E	3400	0.326	44.7

[a] The height of the tan δ peak and [b] The tan δ peak temperature

Table (2) presents a summary of the disc diffusion data for the four samples (A) PVA/0.1 FMWCNTS , (B) PVA/0.2 FMWCNTs , (C) PVA/ 0.3FMWCNTs and (D) (PVA/04 /0.5FFMWCNTs).

Sample	Subtilis	E. Coli	P. aeruginosa	S.aureus
PVA/0.1FMWCNTS	15. 1±0.4	15 ± 0.3	15 ± 0.4	15.6 ± 0.3
PVA/0.2FMWCNTS	16.2 ± 0.6	15.44 ± 0.5	15.44 ± 0.6	15.5 ± 0.5
PVA/0.3FMWCNTS	17.5 ± 0.7	16.1 ± 0.4	15.6 ± 0.7	16.8 ±0.6
PVA/0.5FMWCNTS	18.6 ± 0.9	16.6 ± 0.7	16.11±0.6	17.8 ± 0.6

Where antibacterial activity was expressed as diameter of bacterial growth, inhibition zone in presence of PVA/ FMWCNTs nanostructure

DISSCUSSION

Structural evaluations

The FTIR spectra were recorded and presented in Fig 1 to assess the nanofiller synthesis. The signal in the acid functionalized MWNTs spectra at 3450 cm^{-1} indicates the presence of a hydroxyl group on the nanotube surface. A broad band at 3425 cm^{-1} that is indicative of the hydroxyl groups' OH stretching vibration and a carboxylic acid's C=O at 1710 cm^{-1}. At 1625 cm^{-1}, the unoxidized graphitic domain band is seen (**Quintavalla et al., 2002).** The consequence of stretching C-H was recorded at 2928 cm^{-1}. For pure PVA, Fig. 1 A shows two main distinguishing bands (**Joerger et al., 2007 and Silvestre, 2011)**. The first one is caused by the O-H stretching vibration of the PVA hydroxyl groups, which vibrate at 3330 cm^{-1}. It is well known that the O-H and C-OH stretching bands can both be impacted by hydrogen bonding (**Huang et al., 2011).** The band near 3340 cm^{-1} of the pure film shifts to a lower wavenumber, 3330 cm^{-1}, with an increase in the O-H band width and a decrease in intensity upon the addition of nanofillers. This indicates the presence of strong intra- and intermolecular hydrogen bonding between the function groups of the nanofillers and the free hydroxyl groups of PVA (**Wei et al., 2011)**.

When FMWCNTs were added to the pure PVA in two different concentrations 0.2 and 0.5 as lower and higher concentration of FMWCNTs (Fig. 2), the shape of the fracture surface of FMWCNTs was drastically changed (**Azerdo et al., 2013)**. Fig 2 clearly shows a uniformly ordered layered structure of PVA's dispersion. The picture of the nanocomposite was smoother in the lower concentration than the higher concentration, suggesting that the surfaces of FMWCNTS sheets were covered with the PVA polymer. This indicates that there were significant interfacial interactions between PVA and the FMWCNTs **(Tankhiwale et al., 2012)**. The addition of 0.1% functionalized FMWCNTs (sample C) induced an increase in Tg, which reached its highest at 46.05 ^{o}C as a result of stronger hydrogen bonds being formed between the free hydroxyl group of PVA and the carboxylic acid of the functionalized carbon nanotubes. However, for sample (D) shows a bit deviation in the Tg of the PVA at 41.79 ^{o}C and 32.38 ^{o}C for sample (E), respectively. This could be as a result of nanofillers clustering together rather than combining with PVA.

Mechanical evaluations

The DMA experimental results on PVA, and PVA/FMWCNTs nanocomposites were clearly shown in Fig (4) displaying that the glass transition temperature (Tg) of the nanocomposites is much higher than that of pure PVA up to sample (C). When the concentration of FMWCNTs increase the peak transfers to a higher temperature and the relaxation strength decreases, as shown by the results in Table (1) and the tan δ against temperature graphs in Fig (4). This change in the tan δ peak revealing that the polymer chain can't move in segments is because of the nanofillers that have been added. The presence of 'interphase' polymer, which is formed when chains interact with platelet surfaces, has been related to such Tg shifts (**Arfat et al., 2014** and **Joerger et al., 2007)**.

Biological evaluations

Antimicrobial activity

Table (2) presents a summary of the disc diffusion data for the four samples (A) PVA/0.1 FMWCNTS, (B) PVA/0.2 FMWCNTs, (C) PVA/ 0.3FMWCNTs and (D) (PVA/04 /0.5FFMWCNTs). The investigation of antibacterial activity was conducted using the sizes of the clear inhibition zones. The obtained data indicated that pure MWCNT exhibited no antibacterial action against the examined microorganisms. The inhibitory zones for the PVA films with varying MWCNT concentrations were evident. PVA/MWCNT composite is effective against

both Gram-positive and Gram-negative bacteria, according to disc diffusion data. As a result, we can say that the MWCNT-incorporated PVA films demonstrated outstanding antibacterial efficacy against each of the four microorganisms. Subtilis, E.Coli, P. Areoginosa and S.aureus were tested for the PVA/ FMWCNTs nanostructure. For all four pathogens, the PVA films containing MWCNT demonstrated outstanding antibacterial efficacy as shown in table (1) SWCNT significantly inhibit B. Anthracis by damaging and inactivating its cell membrane **Sayed et al. (2024).** However, (SWCNT) significantly inhibit the growth of E. coli by inducing damage to the cell membrane and promoting the release of stress-related gene products.

CONCLUSION

Since the surface of carbon nanotubes is extremely hydrophobic and has negative toxicological effects. In addition to its physicochemical characteristics, such as their length, specific surface area, degree of oxidation, surface topology, bound functional groups, manufacturing process, concentration, and dose given to organisms, are responsible for their toxicity. Here in, this study reports the addition of FMWCNTs is the reason for the change in the tan δ peak, which indicates that the polymer chain cannot move in segments. Subtilis, P.aeroginosa, S. aureus, and E. Coli were examined in relation to the PVA/ FMWCNTs nanostructure. The PVA films incorporating MWCNT showed exceptional antibacterial activity against all four infections.

REFERENCES

Abdullah O. G., and Saleem S. A. 2016, Effect of copper sulfide nanoparticles on the optical and electrical behavior of Poly (vinyl alcohol) films. Journal of Electronic Materials, 45 (11) 5910–5920.

Arfat Y.A., Benjakul S.T, Prodpran, P. Sumpavapol, and P. Songtipya, 2014, Properties and antimicrobial activity of fish protein isolate/fish skin gelatin film containing basil leaf essential oil and zinc oxide nanoparticles. Food Hydrocolloids, 41,265–273.

Azeredo De, H.M.C. Antimicrobial nanostructures in food packaging, 2013, Trends Food Sci Technol, 30, 56–69

Bose S., Kuila T., Mishra A.K., Rajasekar R., Kim N.K. and Le J.H., 2012, Carbon-based nanostructured materials and their composites as supercapacitor electrodes, Journal of Materials Chemistry, 22(3): 767-784.

Coleman J.N. et al., 2004, High performance nanotube-reinforced plastics: Understanding the mechanism of strength increase, Advanced Functional Materials, 14(8): 791-798.

Hemalatha K. S., Rukmani K. , Suriyamurthy N., and Nagabhushana B. M, 2014, Synthesis, characterization and optical properties of hybrid PVA–ZnO nanocomposite: A composition dependent study. Materials Research Bulletin, 51, 438–446.

Huang Y., and Chen H, 2011, Effect of organic acids, hydrogen peroxide and mild heat on inactivation of Escherichia coli O157:H7 on baby spinach. Food Control, 22(8), 1178 –1183.

Joerger R. D., 2007, Antimicrobial films for food applications: a quantitative analysis of their effectiveness. Technol. Sci, 20, 231–273.

Kuang Dai J. Z., Liu L. Z., Yang Jin M., Zhang Z., 2015, Synergistic effects from graphene and carbon nanotubes endow ordered hierarchical structure foams with a combination of compressibility, superelasticity and stability and potential application as pressure sensors, Nanoscale 7 (20) 9252–9260.

Muhammad Q. K., Davood K., Nazish N., Amir S., Tanveer H., Zeeshan K., 2019, Preparation and characterizations of multifunctional PVA/ZnO nanofibers composite membranes for surgical gown application.

Journal of materials research and technology, 8, 1328-1334

Nath, B.C., Gogoi, B.; Boruah, M.; Khannam, M.; Ahmed, G.A.; Dolui, S. K. 2014, High performance polyvinyl alcohol/multi walled carbon nanotube/polyaniline hydrogel (PVA/MWCNT/PAni) based dye sensitized solar cells. Electrochimica Acta, 146: 106-111.

Novaes R., Rurali P. and Ordejon, 2010, Electronic transport between graphene layers covalently connected by carbon nanotubes, ACS Nano 4 (12) :7596–7602.

Palumbo A, Li Z, Yang EH. Trends on carbon nanotube-based flexible and wearable sensors via electrochemical and mechanical stimuli: a review. 2022, IEEE Sens J. 22:20102–25.

Quintavalla S., and Vicini L., 2002, Antimicrobial food packaging in meat industry, Meat Science, 62 (3) 373–380.

Ribeiro H, Schnitzler MC, da Silva WM, Santos AP. 2021 , Purification of carbon nanotubes produced by the electric arc-discharge method. Surf Inter-faces., 26:101389.

Sayed Mohammad Mahdi Dadfar and Gholamreza Kavoosi, 2014, Antibacterial Features, and Water Vapor Permeability of Polyvinyl Alcohol Thin Films Reinforced by Glutaraldehyde and Multiwalled Carbon Nanotube, Polymer composites, 73, 1736-1743

Silvestre C., Duraccio D., and Cimmino S., 2011, Food packaging based on polymer nanomaterials. Progress in Polymer Science, 36(12) 1766–1782.

Stankovich S., et al.,2007, Synthesis of graphene-based nanosheets via chemical reduction of exfoliated graphite oxide. carbon, 45(7): 1558-1565.

Tankhiwale R., and Bajpai S. K., Preparation, characterization and antibacterial applications of ZnO-nanoparticles coated polyethylene films for food packaging. Biointerfaces, 90, 2012, 16–20.

Uddin M.E. et al., 2015, Preparation and properties of reduced graphene oxide/ polyacrylonitrile nanocomposites using polyvinyl phenol. Composites Part B: Engineering, 80, 238-245.

Wei H. Y., Yan Jun L. , Ning Tao and W. LiBing. 2011, Application and safety assessment for nano-composite materials in food packaging. Journal of Materials Science, 12, 1216–1225.

Zhu Y., Li L., Zhang C. G. , Casillas, Z., Sun Z. , Yan G., Ruan Z., Peng A, Raji, C., Kittrell, R.H, Hauge, J.M. 2012, Tour, A seamless three-dimensional carbon nanotube graphene hybrid material, Nat Commun 3 (92) 1–7.